Progress at NIST Toward Absolute Frequency Standards Using Stored Ions

D. J. WINELAND, J. C. BERGQUIST, J. J. BOLLINGER, W. M. ITANO, D. J. HEINZEN,
S. L. GILBERT, C. H. MANNEY, AND M. G. RAIZEN

Abstract—Experiments at NIST, whose goal is to realize frequency standards of high accuracy using stored ions, are briefly summarized. In one experiment, an RF oscillator is locked to a nuclear spin-flip hyperfine transition (frequency $= 3.03 \times 10^8$ Hz) in $^9\text{Be}^+$ ions that are stored in a Penning trap and sympathetically laser-cooled. Stability is better than $3 \times 10^{-12} \, \tau^{-(1/2)}$ and uncertainty in Doppler shifts is estimated to be less than 5×10^{-15}. In a second experiment, a stable laser is used to probe an electric quadrupole transition (frequency $\simeq 1.07 \times 10^{15}$ Hz) in a single laser-cooled $^{199}\text{Hg}^+$ ion stored in a Paul trap. The measured Q value of this transition is approximately 10^{13}. Future possible experiments are also discussed.

INTRODUCTION

ONE GOAL of the ion storage group at NIST (formerly the National Bureau of Standards) has been to realize a stored ion frequency standard whose absolute inaccuracy is less than 1 part in 10^{14}. Primary design considerations in these experiments have been influenced by the assumptions that 1) for many ions in the trap, the uncertainty in the measurement of the second-order Doppler shift will be the largest contribution to inaccuracy and 2) the magnitude of the second-order Doppler shift decreases as the number of ions in the trap decreases.

These assumptions are supported both by experiments and theoretical analysis [1]–[6]. For a given number of ions N in the trap the second-order Doppler shift is minimized when the secular motion in the Paul trap [2]–[5] or the cyclotron and axial motion in the Penning trap [1]–[3] are reduced by some means to negligible values (for example, by the use of buffer gas collisions [4] or laser cooling [6], [7]). For the Paul trap, the second-order Doppler shift is then dominated by the velocity in the RF micromotion [1]–[5]. The basic idea is as follows: in the quadrupole Paul trap the RF micromotion velocity increases with the distance of the ion from the center of the trap. As the number of trapped ions increases, space charge repulsion holds ions farther from the center of the trap thereby increasing the ion's micromotion speed and second-order Doppler shift. For a spherical cloud of ions, the number of ions N is proportional to the fractional sec-

ond-order Doppler shift, averaged over the cloud, $\langle \Delta\nu_{D2}/\nu_0 \rangle$ [2]–[4]:

$$N = -2.16 \times 10^{16} \, r_{cl} M \langle \Delta\nu_{D2}/\nu_0 \rangle / Z^2 \quad (\text{RF trap})$$

$$(1)$$

where r_{cl} is the cloud radius in centimeters, M is the ion mass in atomic mass units and Z is ion charge in units of the proton charge. The number of ions for a given second-order Doppler shift can be increased by using a nonspherical ion cloud geometry in an elongated trap [5]. However, the basic idea still holds that as the number of ions increases so does $|\langle \Delta\nu_{D2}/\nu_0 \rangle|$. The second order Doppler shift is minimized for a single ion [6] or for more than one ion in a trap with linear geometry (discussed below).

In the Penning trap, when the cyclotron and axial kinetic energies are reduced to small values, the second order Doppler shift is dominated by the velocity in the rotation of the ion cloud. In this case, N and $\langle \Delta\nu_{D2}/\nu_0 \rangle$ are related by [1]–[3]

$$N = 3.10 \times 10^{13} \, B \langle -\Delta\nu_{D2}/\nu_0 \rangle^{1/2}$$
$$\cdot z_{cl}(r_{cl} - r'_c)/Z \quad (\text{Penning trap}) \qquad (2)$$

where B is the trap magnetic field strength in teslas, $2z_{cl}$ and r_{cl} are the cloud height and radius in centimeters, $r'_c = (5 \langle -\Delta\nu_{D2}/\nu_0 \rangle)^{1/2} c/\Omega_c$ (Ω_c is the ion's cyclotron frequency and c is the speed of light), and Z is the ion charge in units of proton charge. Equations (1) and (2) are valid for one species of ion in the trap.

Therefore, for both traps, $|\langle \Delta\nu_{D2}/\nu_0 \rangle|$ increases as N increases and we are faced with a compromise in design. For good signal-to-noise ratio (SNR) and therefore good frequency stability, we desire large N. However this increases $|\langle \Delta\nu_{D2}/\nu_0 \rangle|$ and therefore decreases accuracy because of our inability to measure precisely the velocity distributions needed to determine $\langle \Delta\nu_{D2}/\nu_0 \rangle$. This trade-off between stability and accuracy has resulted in different approaches. In the work of one group [4], [8], a stored $^{199}\text{Hg}^+$ ion standard with excellent stability has been realized. In these experiments $N \simeq 2 \times 10^6$ and $\langle \Delta\nu_{D2}/\nu_0 \rangle \simeq -2 \times 10^{-12}$, so an accuracy of 10^{-14} would require a knowledge of $\langle v^2 \rangle$ to 0.5% precision. This problem can be reduced in the elongated trap geometry of [5] but, in-

dependent of the trap geometry, the accuracy can generally be improved by using smaller numbers.

At NIST the primary goal of stored-ion frequency standard work has been high accuracy. The preceding arguments have forced us to use small numbers of ions (approximately 10^4 or less) that are laser-cooled. The loss in short-term stability due to reduced numbers can be partially regained by going to very long interrogation times. These trade-offs are apparent from the expression for stability if we assume the Ramsey method of interrogation and assume 100% detection efficiency. For these conditions [3],

$$\sigma_y(\tau) = (\tau N T_R \omega_0^2)^{-(1/2)} \quad (\tau > T_R) \qquad (3)$$

where τ is the averaging time, T_R is the Ramsey interrogation time and ω_0 is the clock transition frequency (in radians per second). From this expression, we also see the importance of making ω_0 large.

Of course, to achieve high accuracy, we must also account for the perturbations due to static and time-varying multipole interactions for electric, magnetic, and gravitational fields. These include atom-trap field interactions, collisions, shifts due to uncontrolled electric and magnetic fields, and gravitational red shifts. However for more than one ion in the trap, the dominant uncertainty appears to be caused by the uncertainty in the second-order Doppler shift.

Below, we briefly discuss experiments at NIST on stored-ion frequency standards. More detailed accounts are forthcoming.

^{9}Be$^+$ Hyperfine Clock

In this experiment, an oscillator has been locked to the $(m_I = -1/2, m_J = 1/2) \leftrightarrow (-3/2, 1/2)$ nuclear spin-flip hyperfine "clock" transition $(\omega_o/2\pi \cong 303 \text{ MHz})$ in the ground state of ^{9}Be$^+$ (Fig. 1). The basic idea of this experiment has been described previously [9]–[12]; the current experiment works as follows [12]: Between 5000 and 10 000 ^{9}Be$^+$ ions and 50 000 to 150 000 ^{26}Mg$^+$ ions were simultaneously stored in a cylindrical Penning trap [12] with $B \cong 0.8194$ T under conditions of high vacuum ($\leq 10^{-8}$ Pa). At a magnetic field B of 0.8194 T the clock transition depends only quadratically on magnetic field fluctuations, and therefore the accuracy is not limited by field fluctuations. To minimize second order Doppler shifts of the clock transition, the ^{9}Be$^+$ ions were cooled to less than 250 mK in the following manner: The ^{26}Mg$^+$ ions were directly laser-cooled and compressed by a narrow-band (~ 1 MHz) laser radiation source at 280 nm. The ^{9}Be$^+$ ions were then sympathetically cooled [13] by their Coulomb interaction with the cold Mg$^+$ ions (see Appendix I). A narrow-band 313-nm radiation source was used to optically pump and detect the ^{9}Be$^+$ ions [9]–[12]. With the 313-nm source tuned to the $2s \, ^2S_{1/2}(m_I = 3/2, m_J = 1/2)$ to $2p \, ^2P_{3/2}(3/2, 3/2)$ transition, 94% of the ^{9}Be$^+$ ions were optically pumped into the $2s \, ^2S_{1/2}(3/2, 1/2)$ ground state. The 313-nm source was then turned

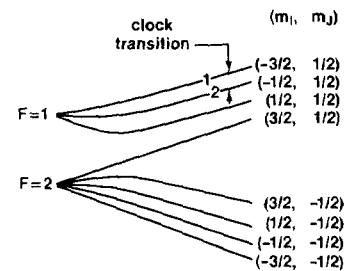Fig. 1. Hyperfine energy levels (not drawn to scale) of the ^{9}Be$^+$ $2s \, ^2S_{1/2}$ ground state as a function of magnetic field. At $B = 0.8194$ T the 303 MHz clock transition is independent of magnetic field to first order.

off to avoid optical pumping and ac Stark shifts while the clock transition was driven.

The clock transition was detected by the following method: After the 313-nm source was turned off, the ions in the (3/2, 1/2) state were transferred to the (1/2, 1/2) state and then to the ($-1/2$, 1/2) state by two successive RF π pulses. Each pulse was 0.2 s long and was resonant with the appropriate transition frequency (around 321 MHz and 311 MHz respectively). The clock transition was then driven by Ramsey's method of separated oscillatory fields in the time domain with RF pulses of about 1-s duration and a free precession time on the order of 100 s. This transferred some of the ions from the ($-1/2$, 1/2) state to the ($-3/2$, 1/2) state. Those ions remaining in the ($-1/2$, 1/2) state were then transferred back to the (3/2, 1/2) state by reversing the order of the two RF π pulses. The 313-nm source was then turned back on, and the population of ions in the ($-3/2$, 1/2) state was registered as a decrease in the ^{9}Be$^+$ fluorescence, relative to the steady-state fluorescence, during the first second that the 313-nm source was on. (The optical repumping time of the ions from the ($-3/2$, 1/2) state to the (3/2, 1/2) state was about 10 s.) The sympathetic cooling of the ^{9}Be$^+$ ions by the continuously cooled Mg$^+$ ions is necessary if long interrogation times are to be used, since otherwise the ^{9}Be$^+$ ions would slowly heat up while the 313-nm laser is off [11].

The Ramsey signal was used to steer the frequency of a synthesized RF source [9]–[12]. Ramsey signal measurements were taken near the frequencies corresponding to the half minimum points on both sides of the center frequency. The difference in the measured signal strengths on either side of the line center was used to electronically steer the average frequency of the synthesizer to ω_0. Most runs were taken with a commercial cesium beam clock (fractional frequency stability $\sigma_y(\tau) \cong 6 \times 10^{-12} \tau^{-(1/2)}$ for measurement time τ in seconds) as the reference oscillator, but a few runs were taken with a passive hydrogen maser $(\sigma_y(\tau) \cong 2\text{--}3 \times 10^{-12} \tau^{-(1/2)})$ as the reference oscillator. Stabilities of the ^{9}Be$^+$ clock are measured to be better than $3 \times 10^{-12} \tau^{-(1/2)}$ for the number of ions used, which is within a factor of 4 of the theoretical maximum stability given by (3). The systematic offset of our measurement due to the second-order Doppler frequency shift was dominated by the velocity in the rotation motion

of the ions about the trap axis. This shift was measured to be $(-1.2 \pm 0.5) \times 10^{-14}$.

An apparent pressure shift with an unexpectedly large value was discovered when the background gas pressure was increased. The background gas pressure could be increased by moving the magnet of the sputter ion pump that evacuated the trap region so that it overlapped fewer pumping cells and reduced the pumping speed. (We checked to make sure the magnetic field at the site of the ions was not disturbed.) The composition of the gas was not known since the pressure was measured with a Bayard–Alpert gauge. However, when the vacuum vessel containing the trap was initially evacuated the dominant background gases were H_2 and He as determined by a quadrupole mass analyzer. Therefore we expect that the background gas during the frequency standard measurements was either H_2 or He, or both. If the background gas was dominated by He, the fractional pressure shift was measured to be about -3×10^{-6} Pa^{-1}; if the background was dominated by H_2, the pressure shift was measured to be about -9×10^{-6} Pa^{-1}. Atomic ion hyperfine pressure shifts for He have previously been measured in $^{137}Ba^+$ [14] and in $^{199}Hg^+$ [8] to be 5×10^{-11} Pa^{-1} and 4×10^{-11} Pa^{-1} respectively. The authors of [14] show that the charge induced multipole interaction between the Ba^+ and the noble gas atoms used in that study should give an important contribution to the pressure shift. Since this interaction depends primarily on the polarizability of the neutral we would expect that the pressure shift for He atoms on $^9Be^+$ ions would not be significantly different than that for Ba^+ or Hg^+. Similarly, since the polarizability of H_2 is midway between Ar and Ne, we might expect the pressure shift for H_2 on Be^+ to be near those for Ar and Ne on Ba^+, which were measured to be -6×10^{-10} Pa^{-1} and -6×10^{-9} Pa^{-1} respectively.

The apparent large discrepancy between our data and other measured pressure shifts is not understood at this time. One possible explanation is suggested by studies [15] of radiative association of C^+ with H_2 to form CH_2^+. In the models of this process, it is assumed that the H_2 can stick to the C^+ for a long enough time to allow the C^+–H_2 complex to radiatively stabilize. This sticking is possible because the collision energy can be taken up by the internal degrees of freedom in the H_2 molecule. The sticking time can be orders of magnitude longer than the interaction time during a simple elastic collision. If a similar sticking mechanism is active in H_2–Be^+ collisions, it may account for the apparent large pressure shift. One way to check this hypothesis is to measure the pressure shifts of Be^+ on Ne and Ar, where the sticking would not be expected to occur, and on H_2 or other polyatomic gases, where sticking might occur.

The uncertainty in this apparent pressure shift will probably limit the accuracy of the current $^9Be^+$ clock measurements to around 1 part in 10^{13}. However, we hope to more fully understand the shift before stating a final uncertainty. We are also continuing to search for other causes of systematic errors such as electronic offsets.

However, we feel the accuracy could be improved beyond 5 parts in 10^{15} in the future. If the apparent collisional shift is real, it may be necessary to use liquid He cryopumping to reduce the background pressure.

Hg^+ OPTICAL CLOCK

The velocity in the micromotion for an ion in a quadrupole RF trap is proportional to the distance of the ion from the center of the trap. For two or more laser-cooled ions in the trap, the Coulomb repulsion between ions holds them away from the trap center, and the second-order Doppler shift is dominated by the velocity of micromotion. However, a single ion can be held near the trap center if sufficiently cooled. In this case the kinetic energy in the micromotion can be equal to that of the secular motion [2], [3], [16], [17]. If the ion is laser-cooled, resulting Doppler shifts can be extremely small; uncertainties can be less than 1 part in 10^{20} in some cases [17], [18]. However with $N = 1$, stability is marginal unless we make ω_0 high enough (see 3). One way to accomplish this is to let ω_0 correspond to an optical transition. Dehmelt suggested this idea in 1973 [6]. The reasons that a clock based on an optical transition in an ion has not been realized yet are: 1) it took several years to isolate and manipulate single ions in the traps; 2) local oscillators (lasers) with the desired spectral purity are still not available; and 3) accurate comparison of laser and microwave frequencies is extremely difficult and remains an important problem. Nevertheless the potential accuracy of single-ion optical frequency standards is extremely high [6], [19] ($\simeq 10^{-18}$) so it is important to pursue this research.

At NIST we have investigated the use of the $5d^{10}6s$ $^2S_{1/2} \rightarrow 5d^96s^2$ $^2D_{5/2}$ electric quadrupole transition ($\omega_0/2\pi \simeq 1.07 \times 10^{15}$ Hz) in $^{198}Hg^+$ (see Fig. 2) as an optical frequency standard [20]. The single mercury ion is confined in a miniature RF trap that has internal dimensions of $r_o \cong 466$ μm and $z_o \cong 330$ μm [20], [21]. The amplitude of the trapping field (frequency $\Omega/2\pi \cong 21$–23 MHz) can be varied to a peak of 1.2 kV. The ion is laser-cooled to a few millikelvins by a few microwatts of CW laser radiation that is tuned below the $^2S_{1/2}$–$^2P_{1/2}$ first resonance line near 194 nm. In order to cool all motional degrees of freedom to near the Doppler cooling limit [7] ($T = \hbar\gamma/2k_B \cong 1.7$ mK) the 194 nm radiation irradiates the ion from 2 orthogonal directions, both of which are at an angle of 55° with respect to the symmetry (z) axis of the trap. The 282-nm radiation that drives the narrow $^2S_{1/2}$–$^2D_{5/2}$ transition is obtained by frequency-doubling the radiation from a narrowband CW ring-dye laser. The frequency of the laser is stabilized by locking it to a stable Fabry-Perot cavity. The frequency of the laser is scanned by an acoustooptic modulator that is driven by a computer controlled synthesizer. Up to a few microwatts of 282 nm radiation could be focussed onto the ion in a direction counterpropagating with one of the 194-nm light beams.

Optical-optical double resonance was used to detect transitions driven by the 282-nm laser from the ion's $^2S_{1/2}$ ground state to the metastable $^2D_{5/2}$ state [20], [21]. The
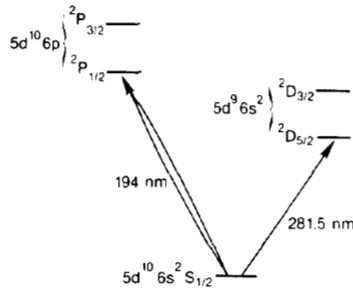
Fig. 2. Simplified optical energy-level diagram for Hg^+. The lifetime of the $^2D_{5/2}$ level is about 0.1 s, which would give a linewidth of approximately 2 Hz on the electric quadrupole $^2S_{1/2} \rightarrow {}^2D_{5/2}$ transition. By observing the presence of or lack of fluorescence from the $^2S_{1/2} \rightarrow {}^2P_{1/2}$ transition, the quadrupole "clock" transition can be detected with 100% efficiency.
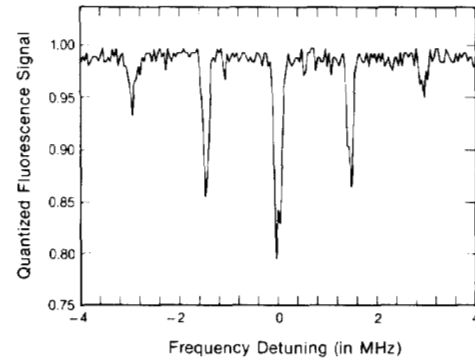

Fig. 3. Quantized signal showing the electric-quadrupole-allowed $5d^{10}6s$ $^2S_{1/2}(m_J = -1/2) \rightarrow 5d^96s^2 {}^2D_{5/2}(m_J = 1/2)$ transition in a single, laser-cooled $^{198}Hg^+$ ion. On the horizontal axis is plotted the relative detuning from line center in frequency units at 282 nm. On the vertical axis is plotted the probability that the fluorescence from the $6s\ ^2S_{1/2}$-$6p$ $^2P_{1/2}$ first resonance transition, excited by laser radiation at 194 nm, is on. The electric-quadrupole-allowed S-D transition and the first-resonance S-P transition are probed sequentially to avoid light shifts and broadening of the narrow S-D transition. Clearly resolved are the recoilless absorption resonance (carrier) and the Doppler sidebands due to the residual secular motion of the laser-cooled ion. Each point is the average of 230 measurement cycles (from [21]).

194-nm fluorescence rate from the laser-cooled ion is high when the ion is cycling between the $^2S_{1/2}$ and $^2P_{1/2}$ states (Fig. 2) and nearly zero when the ion is in the metastable $^2D_{5/2}$ state. The $^2S_{1/2}$-$^2D_{5/2}$ resonance spectrum was obtained by probing the S-D transition at a particular frequency for the 282-nm radiation for 20 ms, then turning off the 282-nm radiation and turning on the 194-nm radiation to look for the presence or absence of scattered photons at 194 nm. (The two radiation fields are alternately applied to avoid light shifts and broadening of the narrow S-D transition by the 194-nm radiation.) If there was no fluorescence at 194 nm, a transition into the metastable D state had occurred; the presence of 194-nm fluorescence indicated that the ion was in the ground state and no transition was recorded for this frequency of the 282-nm laser. The frequency of the 282-nm radiation was then stepped and the measurement cycle repeated. As the frequency was swept back and forth each new result at a particular frequency of the 282-nm radiation was averaged with the previous measurements at that frequency. Normalization (or digitization) of the signal was obtained by assigning a 1 to each measurement of high fluorescence and a 0 to each measurement of no fluorescence. The high fluorescence level made it possible to determine the state of the atom with almost no ambiguity in a few milliseconds. Thus, it is possible to reach the shot noise limit imposed by the single atomic absorber [21].

The quantized fluorescence signal obtained from an 8 MHz scan of the 282-nm laser through the $^2S_{1/2}(m_J = -1/2) \rightarrow {}^2D_{5/2}(m_J = 1/2)$ Zeeman component of the electric quadrupole transition in $^{198}Hg^+$ is shown in Fig. 3. The recoilless-absorption resonance (carrier) and the motional sidebands due to the secular motion in the harmonic well of the RF trap are completely resolved [21].

To avoid broadening of the quadrupole transition due to magnetic field fluctuations, we have recently [22] performed the same experiment on the $^2S_{1/2}(F = 0, m_F = 0) \rightarrow {}^2D_{5/2}(F = 2, m_F = 0)$ transition in $^{199}Hg^+$, which becomes field independent as $B \rightarrow 0$. The carrier is now observed with a linewidth $\Delta\nu \leq 100$ Hz (limited by laser spectral purity), which gives a line Q of about 10^{13}, the highest reported in atomic or molecular spectroscopy.

Current efforts are devoted to improving the 282-nm laser spectral purity by locking it to a more stable reference cavity. If the laser's spectral purity can be made high enough, then when the laser is locked to the ion transition, stabilities are anticipated to be better than 10^{-15} $\tau^{-(1/2)}$ and accuracies could be 1 part in 10^{18} or better [1], [3], [6], [17]–[21].

FUTURE PENNING TRAP EXPERIMENTS

The $^9Be^+$ ion experiments have the primary disadvantage that ω_0 is relatively low and the resulting frequency stabilities are modest. We might hope to substitute $^{201}Hg^+$ ions in place of the $^9Be^+$ ions because $^{201}Hg^+$ has a higher frequency clock transition ($\omega_0/2\pi \cong 26$ GHz), which is field independent at $B = 0.534$ T [1]. However two disadvantages compared to the $^9Be^+$ case arise: (1) If the Hg^+ is sympathetically cooled by lighter ions such as Mg^+ or Cd^+ it will reside in an annulus surrounding the lighter ions [13]; this makes the second-order Doppler shift larger for a given density and number of ions. (2) $^9Be^+$ and $^{25}Mg^+$ have simple optical pumping schemes whereby a single laser frequency can be used to optically pump into a single ground state sublevel [10]. For $^{201}Hg^+$ or $^{199}Hg^+$ in a strong field (required for a Penning trap) optical pumping schemes would require auxiliary laser lines at 194 nm and microwave oscillators to manipulate the ground state sublevels [1]; the simple optical pumping schemes as in the case of $^9Be^+$ and $^{25}Mg^+$ do not appear possible. $^{199}Hg^+$ in a Penning trap would provide a very interesting system when magnets of high enough field strength become available. For example, the ($m_I = 1/2$, $m_J = 1/2$) $\leftrightarrow$ ($-1/2$, $1/2$) hyperfine transition in the ground state of $^{199}Hg^+$ ($\omega_0/2\pi \cong 20.9$ GHz) is field independent at $B = 43.9$ T. At present, we must await the required magnet.

TABLE I
EXPECTED FREQUENCY STABILITIES FOR VARIOUS IONS OF INTEREST FOR FREQUENCY STANDARDS

$M_1(u)$	$M_2(u)$	ω_0	$B(T)$	ξ	$|\Delta\nu_{D2}/\nu_0|$	b_1	z_{cl}(cm)	N_1	T^*	$\sigma_y(1\ s)$ ($T_R = 100$ s)
9(Be⁺)	26(Mg⁺)	303 MHz[10]	0.8194	0.1	10^{-15}	125 μm	0.5	6630	65 mK	6.45×10^{-13}
9(Be⁺)	26(Mg⁺)	303 MHz[10]	0.8194	0.01	10^{-15}	1.25 mm	0.5	67400	65 mK	2.02×10^{-13}
67(Zn⁺)	113(Cd⁺)	1 GHz[23]	8	0.1	10^{-15}	56 μm	0.5	28500	484 mK	9.44×10^{-14}
67(Zn⁺)	113(Cd⁺)	1 GHz[23]	8	0.01	10^{-15}	560 μm	0.5	292000	484 mK	2.94×10^{-14}
199(Hg⁺)	203(Tl⁺)	20.9 GHz	43.9	0.01	10^{-16}	58 μm	0.5	52400	144 mK	3.51×10^{-15}
201(Hg⁺)	203(Tl⁺)	25.9 GHz[1]	0.534	0.1	10^{-15}	1.48 mm	0.5	50100	1.45 K	2.75×10^{-15}
201(Hg⁺)	203(Tl⁺)	25.9 GHz[1]	0.534	0.01	10^{-15}	1.48 cm	0.5	524000	1.45 K	8.49×10^{-16}
201(Hg⁺)	203(Tl⁺)	7.73 GHz[1]	3.91	0.1	10^{-15}	204 μm	0.5	50100	1.45 K	9.21×10^{-15}
201(Hg⁺)	203(Tl⁺)	7.73 GHz[1]	3.91	0.01	10^{-15}	2.04 mm	0.5	524000	1.45 K	2.85×10^{-15}

[a]The ions are assumed to be confined in a Penning trap and sympathetically cooled. M_1 is the mass of the "clock" ion in atomic mass units (u), M_2 is the mass of the ion that is directly laser cooled and sympathetically cools M_1. For all cases $M_1 < M_2$ so that the cloud geometry of Fig. 5 applies. The clock frequency ω_0 is assumed to be "field independent" as for the ^{9}Be⁺ case described in the text. This choice determines the magnetic field. From the magnetic field B and an assumed value of ξ (6), the density of species 1 can be determined from (5). If we desire a certain value of the second order Doppler shift $\langle \Delta\nu_{D2}/\nu_0 \rangle$, we then determine a value of the cloud radius b_1 and the ion number (7) for an assumed value of z_{cl}. From (3), we then determine $\sigma_y(\tau)$ assuming $T_R = 100$ s for the Ramsey interrogation time. We refer to $\sigma_y(1$ s) for convenience. T^* is the temperature at which the second order Doppler shift from the axial and cyclotron motion would be equal to the value listed in the table. Therefore we have implicitly assumed the temperature of the cyclotron and axial motion is much less than T^*. From this, we see the importance of laser cooling.

Within the limits imposed by today's technology, an experiment similar to the ^{9}Be⁺ experiment but with better expected performance might be provided by ^{67}Zn⁺ ions [23]. The clock transition could be the $(m_I = /2, m_J = 1/2) \leftrightarrow (3/2, 1/2)$ transition ($\omega_0/2\pi \simeq 1$ GHz), which is field independent at $B \simeq 8$ T. Some other examples are summarized in Table I. Similar schemes are possible with ions such as Ba⁺ but optical pumping is complicated.

FUTURE PAUL TRAP EXPERIMENTS

The advantage of the Paul trap is that a magnetic field is not required for trapping. This allows us to be rid of a cumbersome magnet and allows use of transitions that are field independent at $B = 0$. The primary disadvantage is that up to the present time it has been impossible to laser-cool very many ions ($N > 100$). As discussed above, the use of small numbers may not be a limitation if ω_0 can be made big enough. This is the basic philosophy behind the single-ion optical frequency standards. Even for $\omega_0/2\pi = 40.5$ GHz (^{199}Hg⁺) and $N = 1$, from (3) we can expect [3] $\sigma_y(\tau) = 3.9 \times 10^{-13}\ \tau^{-(1/2)}$ when $T_R = 100$ s. Because the second-order Doppler shift is expected to be so small for single ions, it is perhaps useful to look at this case a little more closely.

The main advantage of using a single ion in an RF trap is that the kinetic energy of micromotion can be on the order of the secular motion energy. For a single ^{199}Hg⁺ ion cooled to the Doppler-cooling limit [21], the second-order Doppler shift would be [3] $\langle \Delta\nu_{D2}/\nu_0 \rangle = -2.3 \times 10^{-18}$. In a quadrupole ion trap, two or more ions in the trap are pushed from the center of the trap by the mutual Coulomb repulsion and the second-order Doppler shift is higher [2]. Consider the trap shown in Fig. 4. This design is essentially the same as that described by Prestage et al. [5] and Dehmelt [24]. In the trap of Fig. 4, the RF electric fields are transverse to the trap axis for the entire z extent of the trap. If a single string of ions is trapped along the z axis, then the kinetic energy of micromotion is about
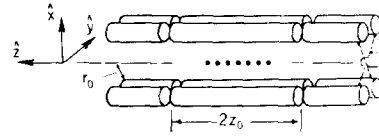

Fig. 4. Linear trap configuration. The alternating RF voltage $V_o \cos \Omega t$ is assumed to be applied to diagonally opposing electrodes as shown. We assume the end portions of the electrodes are long enough that the resulting RF potential at the position of the ions is independent of z, so that the RF electric fields are parallel to the x-y plane. To trap ions along z, we assume the center four electrodes are at static ground potential and the two sets of four electrodes on either end are at a static potential U_o ($U_o > 0$ to trap positive ions). The average position of the ions could be made to coincide with the RF electric field null by applying slightly different static potentials to the four central rods to correct for contact potential offsets etc. This geometry would allow laser beams to be directed along the z axis. Such a trap might also be useful for studing fundamental atom-radiation interactions such as the statistics of fluorescence from or the interaction of a cavity with two or more well localized atoms.

equal to the kinetic energy in the secular motion. Therefore, the fractional second-order Doppler shift could be as low as $5kT/2mc^2$. This is 5/6 of the value for a quadrupole RF trap [2] because of the absence of RF micromotion along the z direction. At the Doppler-cooling limit, this gives $\Delta\nu_{D2}/\nu_0 \simeq -2 \times 10^{-18}$ for all Hg⁺ ions in the string.

Use of the trap of Fig. 4 would allow $N \gg 1$ giving good stability and still yield a small second-order Doppler shift. For the experimentally achievable conditions of Appendix II, $N = 50$ ions could be stored along the z axis like "beads on a string" with ion spacings of approximately 5 μm. With this spacing each ion could be independently detected by using an image detector [25], [26], [39]. Therefore each ion could be treated as an independent atomic clock where the clock transition could be detected with 100% efficiency [21]. From (3), for $T_R = 100$ s and $\omega_0/2\pi = 40.5$ GHz (^{199}Hg⁺) the frequency stability of this clock "ensemble" would be $\sigma_y(\tau) = 5.5 \times 10^{-14}\ \tau^{-(1/2)}$. For these long interrogation times, sympathetic cooling might be required to avoid heating while

the Hg^+ optical pumping laser was turned off to avoid light shifts during the Ramsey period. The ions used to cool the Hg^+ ions would also find a position in the string of ions along the z axis. Arrays of traps have also been proposed previously [27]. These trap arrays would have the same advantages as above for increasing N and minimizing the second-order Doppler shift.

For optical spectroscopy, lasers with high spectral purity are required (see the following). This is the current limitation to reaching the natural linewidth resolution in the NIST Hg^+ experiments. In future experiments, the laser can be locked to the ion resonance line in a manner similar to that described for the $^9Be^+$ hyperfine transition. That is, the clock transition is alternately probed on either side of the resonance (at the frequencies near maximum slope). After several measurements an error signal is built up which is used to servo the average frequency of the laser to the center of the clock resonance. A partial test of this lock can be made by briefly interrupting this servo, probing a portion of the clock resonance line (while assuming that the center of the clock resonance is given by the most recent servo measurements), and then returning to servo operation. This process is repeated until a resonance line similar to that of Fig. 3 is obtained. This, of course, does not test for a slow drift in the ion resonance frequency, but should be a fairly good test of the ability to servo the laser to the clock transition.

The main systematic error for the Hg^+ optical experiment may ultimately be the uncertainty in the shift of clock transition from static electric fields of quadrupole symmetry such as those caused by static potentials applied to the trap electrodes [6]. The basic idea is that the D state of the clock transition has a quadrupole moment that can interact with static fields of quadrupole symmetry to give a shift that must then be measured. Although troublesome, it should be possible to remove this offset from a clock calibration to about the same precision as the measurement precision [3]. Dehmelt has pointed out the advantage of the singly ionized group IIIA atoms in this respect [6]; the interesting clock transitions in these ions are the $^1S_0 \rightarrow {}^3P_0$ intercombination lines that are not shifted by static quadrupole electric fields. However, at low magnetic field these transitions have magnetic field dependence on the order of the nuclear Zeeman effect. Therefore careful control of the magnetic field would be required [6]. At higher fields, field-independent transitions could be used to advantage [28]. A linear trap or trap arrays could be used to increase SNR as described previously. For clock transitions involving a state with a quadrupole moment, such as for Hg^+, the mutual Coulomb interaction between ions would cause an additional quadrupole frequency shift that must be taken into account [29]. For the group IIIA ions, this shift would be absent.

LASERS AND LASER METROLOGY

For optical frequency standards and spectroscopy experiments, the most outstanding current problem is that of

local oscillator (laser) spectral purity. Lasers that are locked to reference cavities have been shown to track the cavity frequency to precisions of much less than 1 Hz [30]. The problem then remains that the length of the cavity and therefore the frequency of the laser are modulated by acoustic noise with deviations typically much greater than 1 Hz. It is desired to make this reference cavity stable enough (frequency deviations less than the linewidth of the optical transition) over the attack time of the servo used to lock the laser to the ion line.

A more general problem is that of cost, power requirements, and complexity of the lasers required for optical pumping and laser cooling. At present, most experiments use near-ultraviolet laser lines provided by gas laser pumped dye lasers that are frequency doubled or summed to give a few microwatts at wavelengths corresponding to certain transitions in various ions. However, this technology may simplify in the coming years. Partly because of efforts by the optoelectronics industry, it is not unreasonable to think that such lasers will be replaced by cheap, high-efficiency solid-state lasers. This is already happening at near-infrared wavelengths where diode lasers are used to optically pump and laser-cool neutral cesium and rubidium atoms.

Finally, we call attention to the problem of frequency metrology that is important in the generation of time from optical frequency standards. The technology to connect the microwave region of the spectrum to the optical spectrum through the use of synthesis chains exists [31]. Other schemes have been proposed and are being worked on [32], [33], [40]. However, this metrology problem is significant and simpler schemes would help realize the full benefits of optical frequency standards.

APPENDIX I
SYMPATHETICALLY COOLED IONS IN A PENNING TRAP

An approximate model of a two species ion plasma in a Penning trap is shown in Fig. 5. To make the problem tractable, we will assume that the species of spectroscopic interest is of lighter mass (species 1) and therefore resides inside species 2, which is directly laser-cooled. The case where species 2 is sympathetically cooled by species 1 [13] could be treated in a similar manner. If we assume $N_1 \ll N_2$, we can approximate the species 1 ions by a cylinder of radius b_1, and height $2z_{cl}$. If we can assume that the cyclotron and axial motion of the ions have been cooled to negligible values, the second-order Doppler shift averaged over ions of species 1 is due to the velocity of cloud rotation and is given by

$$\langle \Delta\nu_{D2}/\nu_0 \rangle = -\omega^2 b_1^2/4c^2, \qquad (4)$$

where ω is the rotation frequency and c is the speed of light. The density of species 1 is

$$n_1 = m_1\omega(\Omega_1 - \omega)/2\pi q_1^2 \qquad (5)$$

where m_1, Ω_1, and q_1, are the mass, cyclotron angular frequency and charge of species 1 [34], [35]. An experimentally useful parameter to characterize the density of spe-
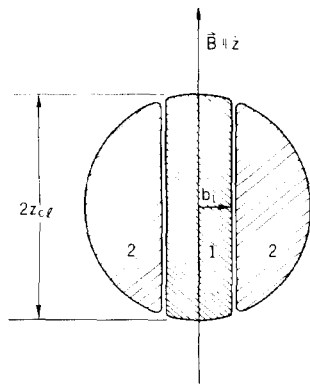
Fig. 5. Approximate model for a sympathetically cooled ion sample in a Penning trap. We assume $q_1/m_1 > q_2/m_2$ so that species 1 (which is the "clock" species) is approximated by a uniform density column of height $2z_{c/}$ and radius b_1. Species 2 is assumed to be continuously laser cooled and by the Coulomb interaction continuously cools species 1. All ions are assumed to be in thermal equilibrium and therefore co-rotate about the z axis at frequency ω. The second order Doppler shift of species 1 is assumed to be dominated by the velocity in this rotation.

cies 2 is the parameter

$$\xi = 2\omega/\Omega_2 \qquad (6)$$

where Ω_2 is the cyclotron frequency of species 2. ξ is the ratio of the rotation frequency ω to the maximum allowable rotation frequency $\Omega_2/2$ given by the Brillouin density [34], [35].

From (4)-(6), and the formula $N_1 = 2\pi b_1^2 z_{c/} n_1$, we have

$$N_1 = 8m_2 c^2 z_{c/}(1 - \xi m_1 q_2/2m_2 q_1)\langle -\Delta\nu_{D2}/\nu_0\rangle/\xi q_1 q_2 \qquad (7)$$

where m_2 and q_2 are the mass and charge of ions of species 2. From these expressions and (3) applied to species 1, we can generate the parameters of Table I. Accuracy of 10^{-15} with reasonable stability seems possible. Of course the local oscillator spectral purity must be good enough to reach these conditions. The $^{199}\text{Hg}^+$ example is not now realistic due to the lack of a suitable magnet.

APPENDIX II
LINEAR PAUL TRAP

To describe the trapping from ponderomotive fields we assume that near the trap axis, the time varying potential has the form

$$\phi = \frac{V_0(x^2 - y^2)}{2R^2} \cos \Omega t \qquad (8)$$

where R is approximately equal to the dimension r_0 indicated in Fig. 4. ($R = r_0$ if the electrode surfaces lie along equipotentials of (8).) If Ω is high enough (defined in the following) this results in the harmonic pseudopotential well in the radial direction:

$$\phi_p = \frac{qV_0^2}{4m\Omega^2 R^4}(x^2 + y^2) = \frac{m}{2q}\omega_r^2(x^2 + y^2) \qquad (9)$$

where $\omega_r \equiv qV_0/(\sqrt{2}\, m\Omega R^2)$ is the single-ion oscillation frequency in the radial direction. Expression (9) is expected to be fairly accurate when $\Omega \gg \omega_r$, which is the condition for Ω being large enough.

For the static potential due to voltage U_0 applied to the end sections, we will make the approximation that, near the center of the trap, this potential is given by

$$\phi_s = kU_0(z^2 - (x^2 + y^2)/2)$$

$$= \frac{m}{2q}\omega_z^2(z^2 - (x^2 + y^2)/2) \qquad (10)$$

where k is a geometric factor and ω_z is the z oscillation frequency for a single ion in the trap. Equation (10) represents the lowest order term in the expansion of the static potential for the electrode configuration of Fig. 4 with the bias assumed. If the length of the central rods is long compared to their spacing, then higher-order terms in the expansion become more important so that the static potential changes significantly only near the point of separation between the end and center sections. For simplicity, we will assume that the length of the central rods is approximately equal to the rod spacing and that the extent of the ion sample is small compared to R so that (10) should be a reasonable approximation to the actual potential.

The addition of this static potential weakens the strength of the pseudopotential well in the radial direction so that the total potential in the radial direction is given by

$$\phi_r = \frac{m}{2q}(\omega_r^2 - \omega_z^2/2)(x^2 + y^2) = \frac{m}{2q}(\omega_r'^2)(x^2 + y^2) \qquad (11)$$

where ω_r' is the single ion radial oscillation frequency for the combined potentials.

A possible advantage of such a linear trap may be for laser-cooling large numbers of ions in an RF trap. As has been noted in recent papers [36], [37], the RF micromotion in a quadrupole Paul trap perturbs the ion's spectrum and can inhibit laser-cooling. This may be one of the main reasons large numbers of ions in an RF trap have not been laser cooled. If a cooling laser is directed along the z axis of the trap in Fig. 4, the ion's spectrum is not perturbed by micromotion and laser cooling should occur according to the simple theory [38], [41] if RF heating is not too severe.

"Beads on a String"

The most interesting case for accurate spectroscopy is when all ions are confined along the z axis. To analyze this case, first assume that ω_r' is large enough to make the ions lie along the z axis. Then, for a given N and ω_z, we minimize the total ion potential to obtain z_i, for $i = (1, \cdots, N)$. From the z_i we can then find a condition on ω_r' to insure all ions stay along the z axis.

For ions pinned on the z axis, the total ion potential

energy is

$$q\phi_T = \frac{m}{2}\,\omega_z^2 \sum_i^N z_i^2 + q^2 \sum_{i<j}^N |z_i - z_j|^{-1} \quad (12)$$

Using a computer, we have minimized ϕ_T as a function of ion positions for various experimental parameters. Near $z = 0$ (trap center), the ions are closest together and fairly regularly spaced. The closer the spacing, the higher ω_r' must be to maintain all ions on the z axis.

To find the condition on ω_r', consider an infinite string of ions with equal spacing d along the z axis. If one ion is displaced a distance $\delta x\,(\ll d)$ from the z axis, it experiences a force away from the z axis of strength

$$F_x = \left(2\sum_{n=1}^\infty n^{-3}\right)\frac{q^2}{d^3}\,\delta x = (2.404)\,\frac{q^2}{d^3}\,\delta x. \quad (13)$$

If we have only 5 ions spaced by d the analogous force on the center ion is given by (13) with the numerical factor equal to 2.250 rather than 2.404. Therefore even if the ions are only approximately evenly spaced, (13) will be a good estimate of F_x for a particular ion if we take d to be the mean of the spacing to the nearest neighbor ions. For the ions to be stably trapped on the z axis, we want the pseudopotential force inward to be larger than the force outward as expressed by (13). From (11) and (13) we therefore require that

$$(\omega_r')^2 > 2.404\, q^2/md^3 \quad (14)$$

or $\omega_r'/2\pi > 91.9\,(Md^3)^{-(1/2)}$ where M is the ion mass in atomic mass units, d is the spacing in micrometers, and $\omega_r'/2\pi$ is in megahertz.

As an example, for $N = 50$, $\omega_z/2\pi = 50$ kHz, and $M = 199$ ($^{199}\mathrm{Hg}^+$ ions), the computer calculation gave an overall string length of 266 μm. The spacings of adjacent pairs of ions in μm, starting from the outermost pair of ions on one end and ending with the center pair are: 10.48, 8.46, 7.43, 6.77, 6.30, 5.95, 5.68, 5.46, 5.28, 5.12, 4.99, 4.88, 4.79, 4.71, 4.64, 4.58, 4.53, 4.48, 4.45, 4.42, 4.39, 4.37, 4.36, 4.35, 4.35. Using $d = 4.35\,\mu$m, we find from (14), $\omega_r'/2\pi > 718$ kHz, $\omega_r/2\pi > 719$ kHz. If $R = 0.75$ mm and $\Omega/2\pi = 5$ MHz, then we require $V_o > 233$ V.

ACKNOWLEDGMENT

REFERENCES

[1] D. J. Wineland, W. M. Itano, J. C. Bergquist, and F. L. Walls, *Proc. 35th Annu. Symp. Freq. Contr.*, Philadelphia, PA, May 1981, pp. 602–611. (Copies available from: Annual Frequency Control Symposium, c/o Electronic Industries Assoc., 2001 Eye St., Washington, DC, 20006.)

[2] D. J. Wineland, "Precision Measurement and Fundamental Constants II," B. N. Taylor and W. D. Phillips, Eds. National Bureau of Standards (U.S.) Spec. Publ. 617 1984, pp. 83–92.

[3] D. J. Wineland, W. M. Itano, J. C. Bergquist, J. J. Bollinger, F. Diedrich, and S. L. Gilbert, in Frequency Standards and Metrology, *Proc. 4th Symp.*, A. DeMarchi, Ed. Berlin: Springer-Verlag, 1989, p. 71–77.

[4] L. S. Cutler, R. P. Giffard, and M. D. McGuire, *Appl. Phys.*, B36, 137, pp. 137–142, 1985; L. S. Cutler, C. A. Flory, R. P. Giffard, and M. D. McGuire, *Appl. Phys.*, vol. B39, pp. 251–259, 1986.

[5] J. Prestage, G. J. Dick, and L. Maleki, *J. Appl. Phys.*, vol. 66, pp. 1013–1017, 1989.

[6] H. G. Dehmelt, *IEEE Trans. Instrum. Meas.*, vol. IM-31, pp. 83–87, 1982, and references therein.

[7] D. J. Wineland and W. M. Itano, *Physics Today*, vol. 40, no. 6, pp. 34–40, 1987.

[8] L. S. Cutler, R. P. Giffard, and M. D. McGuire, *Proc. 37th Annu. Symp. Freq. Contr.*, 1983, pp. 32–36, (copies available from IEEE, 445 Hoes Lane, Piscataway, NJ 08854).

[9] J. J. Bollinger, S. L. Gilbert, W. M. Itano, and D. J. Wineland, in *Frequency Standards and Metrology, Proc. 4th Symp.*, A. DeMarchi, Ed. Berlin: Springer-Verlag, 1989, pp. 319–325.

[10] J. J. Bollinger, W. M. Itano, and D. J. Wineland, *Proc. 37th Annu. Symp. Freq. Contr.*, 1983, pp. 37–41 (copies available from IEEE, 445 Hoes Lane, Piscataway, NJ 08854).

[11] J. J. Bollinger, J. D. Prestage, W. M. Itano, and D. J. Wineland, *Phys. Rev. Lett.*, vol. 54, pp. 1000–1003, 1985.

[12] J. J. Bollinger, D. J. Heinzen, W. M. Itano, S. L. Gilbert, and D. J. Wineland, *Phys. Rev. Lett.*, vol. 63, pp. 1031–1034, 1989.

[13] D. J. Larson, J. C. Bergquist, J. J. Bollinger, W. M. Itano, and D. J. Wineland, *Phys. Rev. Lett.*, vol. 57, pp. 70–73, 1986.

[14] J. Vetter, M. Stuke, and E. W. Weber, *Z. Phys.*, vol. A273, pp. 129–135, 1975.

[15] E. Herbst, *Astrophys. J.*, vol. 252, pp. 810–813, 1982, and references therein.

[16] H. G. Dehmelt, *Adv. At. Mol. Phys.*, vol. 3, pp. 53–72, 1967.

[17] D. J. Wineland, W. M. Itano, J. C. Bergquist, and R. G. Hulet, *Phys. Rev.*, vol. A36, pp. 2220–2232, 1987.

[18] F. Diedrich, J. C. Bergquist, W. M. Itano, and D. J. Wineland, *Phys. Rev. Lett.*, vol. 62, pp. 403–406, 1989.

[19] D. J. Wineland, *Science*, vol. 226, pp. 395–400, 1985.

[20] J. C. Bergquist, F. Diedrich, W. M. Itano, and D. J. Wineland, in *Frequency Standards and Metrology, Proc. 4th Symp.*, A. DeMarchi, Ed. Berlin: Springer-Verlag, pp. 287–292.

[21] J. C. Bergquist, W. M. Itano, and D. J. Wineland, *Phys. Rev.*, vol. A36, pp. 428–430, 1987.

[22] J. C. Bergquist, F. Diedrich, W. M. Itano, and D. J. Wineland, in *Laser Spectroscopy IX*, M. S. Feld, J. E. Thomas, and A. Mooradian, Eds. San Diego, Academic, 1989, pp. 274–277.

[23] W. M. Itano and D. J. Wineland, *Bull. Am. Phys. Soc.*, vol. 24, p. 1185 (1979).

[24] H. G. Dehmelt, in *Frequency Standards and Metrology, Proc. 4th Symp.*, A. DeMarchi, Ed. Berlin: Springer-Verlag, 1989, p. 286.

[25] D. J. Wineland, W. M. Itano, J. C. Bergquist, S. L. Gilbert, J. J. Bollinger, and F. Ascarrunz, in "Non-neutral plasma physics," C. W. Roberson and C. F. Driscoll, Ed. *A.I.P. Conf. Proc.*, vol. 175, Amer. Inst. of Physics, New York, 1988, pp. 93–108.

[26] R. Blümel, J. M. Chen, F. Diedrich, E. Peik, W. Quint, W. Schleich, Y. R. Shen, and H. Walther, in *Atomic Physics*, vol. 11, S. Haroche, J. C. Gay and G. Grynberg, Eds. Singapore: World Scientific, 1989, pp. 243–259.

[27] F. G. Major, *J. de Physique (Lettres)*, vol. 38, pp. L-221–L-225, 1977.

[28] D. J. Wineland and W. M. Itano, *Bull. Am. Phys. Soc.*, vol. 27, p. 864, 1982.

[29] D. J. Wineland, W. M. Itano, J. C. Bergquist, J. J. Bollinger, and J. D. Prestage, *Ann. Phys. Fr.*, vol. 10, pp. 737–748, 1985.

[30] D. Hils and J. L. Hall, in *Frequency Standards and Metrology, Proc. 4th Symp.*, A. DeMarchi, Ed. Berlin: Springer-Verlag, 1989, pp. 162–173.

[31] See, for example, *Frequency Standards and Metrology, Proc. 4th Symp.*, A. DeMarchi, Ed. Berlin: Springer-Verlag, 1989.

[32] D. J. Wineland, J. C. Bergquist, W. M. Itano, F. Diedrich, and C. S. Weimer, in *The Hydrogen Atom*, G. F. Bassani, M. Inguscio, and T. W. Hänsch, Eds. Berlin: Springer-Verlag, 1989, pp. 123–133.

[33] H. R. Telle, D. Meschede, and T. W. Hänsch, *Optics Lett.*, vol. 15, pp. 532–534, 1990.

[34] T. M. O'Neil, *Phys. Fluids*, vol. 24, pp. 1447–1451, 1981.

[35] L. R. Brewer, J. D. Prestage, J. J. Bollinger, W. M. Itano, D. J. Larson, and D. J. Wineland, *Phys. Rev.*, vol. A38, pp. 859–873, 1988.

[36] R. G. DeVoe, J. Hoffnagle, R. G. Brewer, *Phys. Rev.*, vol. A39, pp. 4362–4365, 1989.

[37] R. Blümel, C. Kappler, W. Quint, and H. Walther, *Phys. Rev.*, vol. A40, pp. 808–823, 1989.

[38] D. J. Wineland and W. M. Itano, *Phys. Rev.*, vol. A20, pp. 1521–1540, 1979.

[39] W. M. Itano, J. C. Bergquist, and D. J. Wineland, in *Proc. Workshop on Crystalline Ion Beams*, Wertheim, West Germany, R. W. Hasse, I. Hofmann, D. Liese, Eds., (GSI rep. GSI-89-10, ISSN 0170-4546), pp. 241–254.

[40] T. W. Hänsch, in *The Hydrogen Atom*, G. F. Bassani, M. Inguscio, and T. W. Hänsch, Eds. Berlin: Springer-Verlag, 1989, pp. 93–102.

[41] W. M. Itano and D. J. Wineland, *Phys. Rev.*, vol. A36, pp. 35–54, 1982.

D. J. Wineland, photograph and biography not available at time of publication.

J. C. Bergquist, photograph and biography not available at time of publication.

J. J. Bollinger, photograph and biography not available at time of publication.

W. M. Itano, photograph and biography not available at time of publication.

D. J. Heinzen, photograph and biography not available at time of publication.

S. L. Gilbert, photograph and biography not available at time of publication.

C. H. Manney, photograph and biography not available at time of publication.

M. G. Raizen, photograph and biography not available at time of publication.